Time-Domain Near-Field Analysis of Short-Pulse Antennas—Part II: Reactive Energy and the Antenna Q

Amir Shlivinski and E. Heyman

***Abstract*— The time-domain (TD) multipole expansion, developed in the first part of this two-part sequence, is extended here to analyze the power-flow and energy balance in the vicinity of a pulsed antenna. Using the spherical transmission line formulation, we derive expressions for the pulsed power-flow and energy and identify the radiative and the reactive constituents. For time-harmonic fields, the reactive concepts are well understood in terms of the stored energy, but this interpretation is not applicable for short-pulse fields where there is no stored energy. By considering the TD energy balance, we clarify the transition of the near-zone pulsed reactive energy to the radiation power and show that the pulsed reactive energy discharges back to the source once the pulse has been radiated. We thus introduce a TD Q factor that quantifies the radiation efficiency. In particular, we show that super resolution using short-pulse fields involves large TD reactive energies and Q and is, therefore, not feasible. The general TD concepts discussed are demonstrated through a numerical example of radiation from a circular disk carrying a pulsed current distribution.**

***Index Terms*—Antenna theory, near field, Q factor, short-pulse electromagnetics, time-domain analysis.**

I. Introduction

In Part I [1] of this two part paper, we developed a time-domain (TD) multipole expansion describing the radiation by short-pulse antennas. It has been shown that outside the source domain, the field is completely described by the TD multipole functions which are calculated directly from the time-dependent source distribution. We have also established bounds on the series convergence rate and on the field structure in the near and far zones. In the present work, the emphasis is on the TD representation and analysis of the pulsed power flow and energy and on the resulting antenna properties. We derive closed-form expressions for the TD power-flow and energy and thus identify the TD "radiative" and "reactive" power flow and energy (Section III). For time-harmonic fields, the reactive energy concept is well understood in terms of the stored energy, but it has not been defined yet for time-dependent fields where no stored energy is involved. By considering the TD energy balance, we also clarify the transition of the pulsed reactive energy that dominates in the near zone to the pulsed radiative power in the far zone. It is shown that the strong reactive energy pulse discharges back to the source once the pulse has been radiated. Thus, in order to quantify the effect of the TD reactive energy and on the radiation efficiency, we introduce in Section IV a TD Q which generalizes a similar frequency domain (FD) concept [2]–[6].

The TD concepts discussed above are demonstrated in Section V through a numerical example of radiation from a uniform current pulse on a circular disk, which has been studied in [1] in connection with the calculation of the TD multipole moments and fields. We calculate the TD radiative and reactive energies and the TD Q utilizing the numerical results of [1]. In particular, we calculate these constituents as a function of the normalized source size a/cT where a is the source size and T is the pulse length. Using this example, we also demonstrate that the realization of the field of a large source using a smaller source requires large reactive energy and Q and, therefore, is not feasible.

Throughout the paper we shall refer to equations, sections, and figures from [1], and shall use the prefix I to denote these references [e.g., [1, eq. (3)] is denoted here as (I.3)].

II. Time-Domain Multipole Expansion

This section summarizes of the main concepts and results from [1]. We consider the radiation from a time-dependent source distribution $\mathbf{J}(\mathbf{r}, t)$ bounded by a sphere of radius a. The propagation domain may have a general spherical symmetry, i.e., it may be spherically stratified with $\epsilon(r)$ and $\mu(r)$ and bounded by a general conical surface $\mathcal{C}(\theta, \phi)$ whereon the boundary conditions are imposed. Utilizing the conventional spherical coordinates system $\mathbf{r} = (r, \theta, \phi)$, the field is expressed by the spherical mode expansion in (I.2), which involves both E- and H-type modes, denoted by the superscripts $\alpha = e$ or h, respectively, with ν denoting the mode index. The functions Φ_ν^α, $\mathbf{e}_\nu^\alpha$, and $\mathbf{h}_\nu^\alpha$ are the scalar and vector eigenfunctions that are determined in [1, sec. II]: They depend only on (θ, ϕ) and on the cross-sectional geometry but not on (r, t). The mode amplitudes V_ν^α and I_ν^α, on the other hand, depend only on (r, t) and are found from the spherical wave equations [1, sec. II-B] wherein the source functions i_ν^α and v_ν^α are found from $\mathbf{J}(\mathbf{r}, t)$ via (I.8).

For radiation in free-space, the eigenfunctions are the scalar and vector spherical harmonics in (I.9) and (I.11) with $\nu = (n, m, s)$ being a triple index. Outside the source domain $(r > a)$, the solutions of the spherical transmission line equations (the mode amplitudes) are expressed in (I.13) and (I.15),

Manuscript received September 30, 1997; revised May 4, 1998. This work was supported in part by the U.S. Air Force Office of Scientific Research under Grant 96-1-0039 and by the Israel Science Foundation under Grants 574/95 and 404/98.

The authors are with the Department of Electrical Engineering—Physical Electronics, Tel-Aviv University, Tel-Aviv, 69978 Israel.

Publisher Item Identifier S 0018-926X(99)03735-7.

where the "TD multipole moments" $M_\nu^\alpha(t)$ are calculated from $\mathbf{J}(\mathbf{r}, t)$ via (I.22) and the integral operators $\mathcal{L}_n^{(1,2)}$ are defined in (I.14) and (I.16). The final field solutions expressed explicitly in terms of $M_\nu^\alpha(t)$ are given in (I.17). Alternatively, it might be convenient to express the field in terms of the functions $m_\nu^\alpha(t) = \partial_t^{-N^\alpha} N_\nu^\alpha(t)$ where $N^\alpha = n$ or $n+1$ for $\alpha = e$ or h: $m_\nu^\alpha(t)$ are the integral part in (I.22), and the expressions for the field are now given in (I.19) and involve the differential operators $\hat{\mathcal{L}}^{(1,2)}$. Finally, the large n convergence of the series has been explored in [1, sec. III-D].

The $\tau = t - r/c$ dependence of the solutions in (I.13) and (I.15) describes the outgoing nature of these solutions. Yet for each n, only the $l = 0$ term in the series for $\mathcal{L}_n^{(1,2)}$ propagates with pure delay and without decay or distortion. When substituted in (I.2), this term describes the dominant r^{-1} field term as $r \to \infty$ [see also (I.20)–(I.21) for the TD radiation pattern]. The $l \geq 1$ terms, on the other hand, behave like r^{-l-1} and, therefore, vanish in the far zone but contribute to what will be identified here as the "TD reactive field" in the near zone. Thus, the large n modes have relatively large reactive components in the near zone. As will be explored below, this sets bounds on the order n of the multipoles that can be excited by an antenna with a given support a and, thus, on the antenna gain.

III. TD Energy and Power-Flow

A. The Pulsed Power Flow

The radial power flow with respect to a sphere of radius r is defined as

$$P(r, t) = \oiint_S r^2 \, d\Omega \, \hat{\mathbf{r}} \cdot [\mathbf{E}(\mathbf{r}, t) \times \mathbf{H}(\mathbf{r}, t)] \tag{1}$$

where $\mathbf{E} \times \mathbf{H}$ is the time dependent Poynting vector. Using the modal representation (I.2) and the mode orthonormality [see (I.5)], P may be expressed as a sum of modal powers

$$P(r, t) = \sum_{\alpha, \nu} P_\nu^\alpha(r, t), \qquad P_\nu^\alpha(r, t) = V_\nu^\alpha(r, t) I_\nu^\alpha(r, t). \tag{2}$$

Using (I.13)–(I.16) for V_ν^α and I_ν^α we obtain

$$P_\nu^\alpha = \eta^{\pm 1} \sum_{\ell=0}^{n} \sum_{q=0}^{n+1} a_{n,l} b_{n,q} \left(\frac{c}{r}\right)^{q+\ell} [\partial_t^{-l} M_\nu^\alpha(\tau)][\partial_t^{-q} M_\nu^\alpha(\tau)] \tag{3}$$

where here and henceforth the upper and lower signs are used for the E and H modes, respectively. Arranging the summation as an ascending series of powers of r, it may be expressed as

$$P_\nu^\alpha = P_{\nu_{\text{rad}}}^\alpha(\tau) + P_{\nu_{\text{react}}}^\alpha(r, t) \tag{4}$$

where $P_{\nu_{\text{rad}}}^\alpha$ is the lowest order term while $P_{\nu_{\text{react}}}^\alpha$ represents all other terms. They are given by

$$P_{\nu_{\text{rad}}}^\alpha(\tau) = \eta^{\pm 1} [M_\nu^\alpha(\tau)]^2 \tag{5}$$

$$P_{\nu_{\text{react}}}^\alpha(r, t) = \eta^{\pm 1} \sum_{p=1}^{2n+1} \left(\frac{c}{r}\right)^p \sum_{q=q_{\min}}^{q_{\max}} a_{n,p-q} b_{n,q} \cdot [\partial_t^{q-p} M_\nu^\alpha(\tau)][\partial_t^{-q} M_\nu^\alpha(\tau)] \tag{6}$$

where $q_{\min} = \max\{0, p-n\}$ and $q_{\max} = \min\{n+1, p\}$ (i.e., for $p \in (1, n)$ q goes from zero to p while for $p \in (n+1, 2n+1)$ it goes from $p-n$ to $n+1$).

The leading order term $P_{\nu_{\text{rad}}}^\alpha(\tau)$ is the modal "TD radiative power": It is always positive and, being a function of τ only, it propagates without distortion or decay all the way to infinity. The remainder term $P_{\nu_{\text{react}}}^\alpha(r, t)$ is denoted as the "TD reactive power flow": It vanishes at infinity and for any finite r it has a zero mean, i.e.,

$$\int_{-\infty}^{\infty} dt \, P_{\nu_{\text{react}}}^\alpha(r, t) = 0. \tag{7}$$

This property will also be proved in the Appendix [via a direct analysis of (6)] and will also be verified in (18) from the point of view of energy conservation.

Relation (7) implies that the radiated energy is described only by $P_{\nu_{\text{rad}}}^\alpha$ and is thus independent of r, i.e.,

$$\mathcal{E}_\nu^\alpha = \int_{-\infty}^{\infty} dt \, P_\nu^\alpha(r, t) = \int_{-\infty}^{\infty} dt \, P_{\nu_{\text{rad}}}^\alpha(\tau). \tag{8}$$

Furthermore, as will also be shown in Section III-C (see also numerical example in Section V), the pulsed reactive power flow is initially positive and then has several oscillations so that finally (7) is satisfied. The positive part in $P_{\nu_{\text{react}}}^\alpha(r, t)$ describes power transmitted from the source to build up the local reactive energy while the negative part indicates energy transmitted back to the source as the pulsed field passes over the observation point. This behavior will be clarified further in connection with the conservation of energy relation (17) between the power flow and the energy density.

The functional form of $P_{\nu_{\text{react}}}^\alpha$ implies that in the "near zone" $P_{\nu_{\text{react}}}^\alpha \gg P_{\nu_{\text{rad}}}^\alpha$, so that while the total power flow there is strong only a fraction of it is used for the radiation power. In the "far zone," on the other hand, $P_{\nu_{\text{react}}}^\alpha$ vanishes as $r \to \infty$. Following the analysis of [1, sec. III-D], the modal transition from the near to far zone occurs at $r \sim O(n^2 cT)$. Thus, the reactive zone of the large n modes extends well beyond the source support a. Recalling (I.28), however, these modes are weakly excited. Thus, considering the bounds on the multipole moments, it follows that for the large n modes $P_{\nu_{\text{react}}}^\alpha$ is well behaved and is bounded by $(a/r)^{2n+1}$ for all $r > a$.

B. The Pulse-Energy Density

The magnetic and electric pulsed-energy densities in a spherical shell of radius r (i.e., densities per unit of radius) are defined as

$$w_m(r, t) = \oiint d\Omega \, r^2 \, \tfrac{1}{2} \mu |\mathbf{H}(\mathbf{r}, t)|^2$$

$$w_e(r, t) = \oiint d\Omega \, r^2 \, \tfrac{1}{2} \epsilon |\mathbf{E}(\mathbf{r}, t)|^2 \tag{9}$$

and the *total* energy is $w(r, t) = w_m(r, t) + w_e(r, t)$.

Performing the surface integration in (9) and using mode orthogonality, the pulsed-energy densities can be expressed as a sum of the modal energies

$$w_m(r,t)=\sum_{\alpha,\nu} w^{\alpha}_{m_\nu}(r,t),\quad w_e(r,t)=\sum_{\alpha,\nu} w^{\alpha}_{e_\nu}(r,t) \tag{10}$$

where for E modes

$$w^{e}_{m_\nu}(r,t)=\tfrac{1}{2}\,\mu I^{e2}_{\nu} \tag{11a}$$
$$w^{e}_{e_\nu}(r,t)=\tfrac{1}{2}\,[\epsilon V^{e2}_{\nu}+\epsilon^{-1}r^{-2}n(n+1)(\partial_t^{-1}I^{e}_{\nu})^2] \tag{11b}$$

and for H modes

$$w^{h}_{m_\nu}(r,t)=\tfrac{1}{2}\,[\mu I^{h2}_{\nu}+\mu^{-1}r^{-2}n(n+1)(\partial_t^{-1}V^{h}_{\nu})^2] \tag{12a}$$
$$w^{h}_{e_\nu}(r,t)=\tfrac{1}{2}\,\epsilon V^{h2}_{\nu}. \tag{12b}$$

Note that the terms containing ∂_t^{-1} are due to the longitudinal field components (i.e., E_r and H_r for the E and H modes, respectively). The *total* modal energy densities $w^{\alpha}_{\nu}(r,t)=w^{\alpha}_{m_\nu}(r,t)+w^{\alpha}_{e_\nu}(r,t)$ for the E and H modes are given now by

$$w^{\alpha}_{\nu}(r,t)=\frac{\eta^{\pm 1}}{2c}\,\{[\mathcal{L}^{(1)}_n M^{\alpha}_{\nu}(\tau)]^2+[\mathcal{L}^{(2)}_n M^{\alpha}_{\nu}(\tau)]^2 +n(n+1)(c/r)^2[\partial_t^{-1}\mathcal{L}^{(1)}_n M^{\alpha}_{\nu}(\tau)]^2\} \tag{13}$$

where we have also substituted the expressions for V^{α}_{ν} and I^{α}_{ν} from (I.13) and (I.15). Rearranging terms, separating the part that does not decay with r from the rest, we express (13) as

$$w^{\alpha}_{\nu}(r,t)=c^{-1}P^{\alpha}_{\nu_{\rm rad}}(\tau)+w^{\alpha}_{\nu_{\rm react}}(r,t) \tag{14}$$

where $P_{\nu_{\rm rad}}$ is the modal radiative power defined in (5). Following (4), the reminder is termed the "modal reactive energy" $w^{\alpha}_{\nu_{\rm react}}(r,t)$. An explicit expression for $w^{\alpha}_{\nu_{\rm react}}(r,t)$ involving a series of inverse powers of r is given by

$$w^{\alpha}_{\nu_{\rm react}}(r,t)=c^{-1}P^{\alpha}_{\nu_{\rm react}}(r,t)+\frac{\eta^{\pm 1}}{c}\sum_{p=1}^{2n+1}\left(\frac{c}{r}\right)^{p+1}\sum_{q=q_{\min}}^{q_{\max}} \cdot pa_{n,p-q}b_{n,q}\partial_t^{-1}\{[\partial_t^{q-p}M^{\alpha}_{\nu}(\tau)][\partial_t^{-q}M^{\alpha}_{\nu}(\tau)]\} \tag{15}$$

where the upper and lower signs are for the E and H modes, respectively, while $P^{\alpha}_{\nu_{\rm react}}$, $q_{\min}$ and $q_{\max}$ are defined in (6).

The first term in (14) is identifies as the "TD radiative energy" associated with the radiated power flow $P^{\alpha}_{\nu_{\rm rad}}$. The remainder, $w^{\alpha}_{\nu_{\rm react}}$, describes a local build up of the pulsed energy which accompanies the radiative power, but decays as the pulse is transmitted. As will be discussed in (17) below, part of it is transmitted back to the source. Note that in the near zone $w^{\alpha}_{\nu_{\rm react}}\gg c^{-1}P^{\alpha}_{\nu_{\rm rad}}$, while in the far zone $w^{\alpha}_{\nu_{\rm react}}$ vanishes as $r\to\infty$. The convergence properties of $w^{\alpha}_{\nu_{\rm react}}$ are similar to those of $P^{\alpha}_{\nu_{\rm react}}$, discussed at the end of Section III-A and will not be repeated here.

C. Energy Conservation

Differentiating $P^{\alpha}_{\nu}(r,t)$ in (2) with respect to r and using the transmission line (I.7) we obtain

$$-\frac{\partial}{\partial r}P^{\alpha}_{\nu}(r,t)=\partial_t\, w^{\alpha}_{\nu}(r,t). \tag{16}$$

This relation is readily recognized as the modal analog of the Poynting theorem for the field, which, for $r>a$, is given by $-\nabla\cdot(\boldsymbol{E}\times\boldsymbol{H})=\partial_t(\frac{1}{2}\,\epsilon|\boldsymbol{E}|^2+\frac{1}{2}\,\mu|\boldsymbol{H}|^2)$. In view of (4) and (14) it follows that the relation in (16) is satisfied separately by the radiating and reactive constituent. In particular

$$-\frac{\partial}{\partial r}P^{\alpha}_{\nu_{\rm react}}(r,t)=\frac{\partial}{\partial t}w^{\alpha}_{\nu_{\rm react}}(r,t). \tag{17}$$

This expression clarifies the role of the reactive constituents. At early time $P^{\alpha}_{\nu_{\rm react}}>0$ and describes the local build up of the reactive energy $w^{\alpha}_{\nu_{\rm react}}$, but when $w^{\alpha}_{\nu_{\rm react}}$ discharges, $P^{\alpha}_{\nu_{\rm react}}<0$ and transmits the energy back to the source zone.

Finally, integrating (17), we obtain

$$-\frac{\partial}{\partial r}\int_{-\infty}^{t}dt'\,P^{\alpha}_{\nu_{\rm react}}(r,t')=w^{\alpha}_{\nu_{\rm react}}(r,t) \tag{18}$$

where we used the initial conditions $w^{\alpha}_{\nu_{\rm react}}|_{t=-\infty}=0$. Noting that for a finite duration pulse $w^{\alpha}_{\nu_{react}}\to 0$ as $t\to\infty$ we obtain the result in (7).

D. Example: Energy and Power Flow in the Near and Far Zones

To demonstrate the concepts above, we shall explore in this section the structure of the TD power flow and energy in the near and far zones. We shall calculate these constituents for a synthetic example of a single E mode multipole whose moment $m^{e}_{\nu}(t)$ is a twice differentiate Gaussian pulse (specifically we use the pulse in (I.32): note that unlike the examples in Section V below, the moment function in the present example is not calculate from a given source distribution but it is rather specified analytically). Figs. 1 and 2 depict the radiative and the reactive TD power-flow $P^{e}_{\nu_{\rm rad}}$ and $P^{e}_{\nu_{\rm react}}$ for E mode multipoles of order $n=2$ and $n=5$, respectively, calculated via (5) and (6). The results are shown as a function of $\tau=t-r/c$ for several view points: $r/cT=2,5,10$, and 50.

The near-zone characteristics (dominance of the reactive power flow and energy) are readily observed for $r/cT<n$, whereas for $r/cT\gg n^2$ the field exhibits far-zone characteristics (the reactive power flow and energy vanish and the total pulsed power flow and energy are r independent). The transition zone is identified to be $n<r/cT<n^2$.

IV. Time-Domain Q Factor

A. The Global and the Modal Q

In this section, we introduce a parameter Q that quantifies the energy properties of the radiator by comparing the total radiative energy with a measure of the total reactive energy. We start by defining the total radiating energy $\mathcal{E}_T$

$$\mathcal{E}_T=\int_{-\infty}^{\infty}dt\,P_{T_{\rm rad}}(t) \tag{19}$$

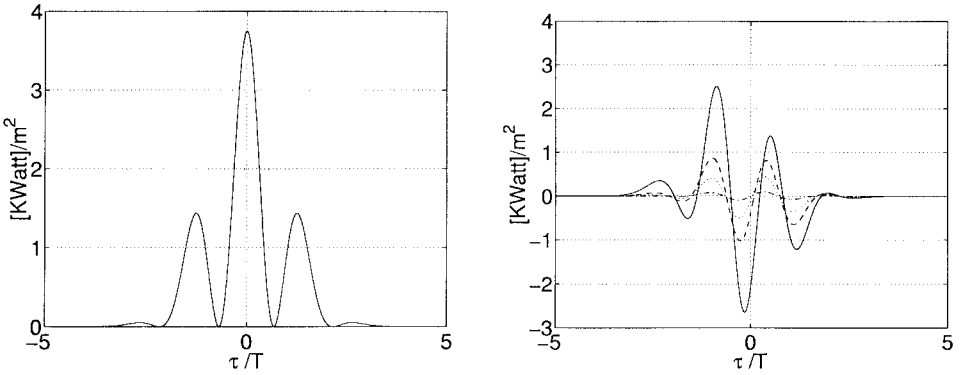

Fig. 1. (a) The radiative and (b) the reactive pulsed power-flow for an E-mode multipole of order $n = 2$. The reactive power is shown as a function of normalized time $\tau/T = (t - r/c)/T$ for several view points: $r/cT = 2, 5, 10,$ and 50 (full, dashed, dotted, and dashed-dotted lines, respectively). The radiative power is unchanged as a function of r.

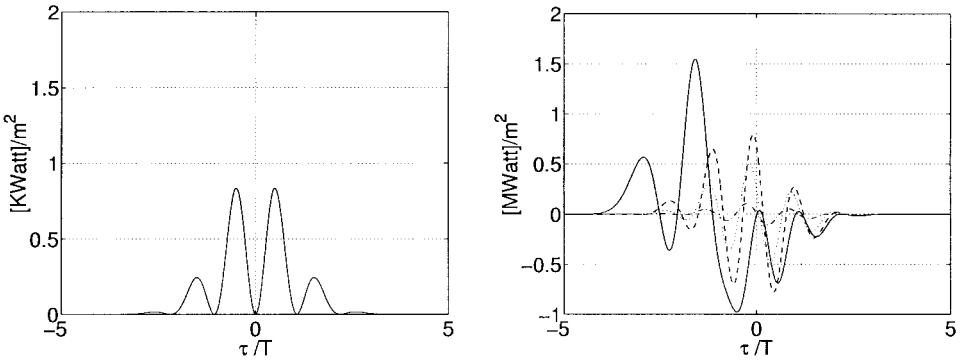

Fig. 2. As in Fig. 1, for an E-mode multipole of order $n = 5$.

where $P_{T_{\rm rad}(t)} = \sum_{\nu,\,\alpha} P^{\alpha}_{\nu_{\rm rad}}(t)$ is the *total* TD radiated power. As a measure for the total reactive energy we use the *time-averaged* reactive energy at $r > a$

$$\mathcal{W}_T(a) = \frac{1}{T_T} \int_a^{\infty} dr \int_{-\infty}^{\infty} dt\, w_{T_{\rm react}}(r,\, t) \tag{20}$$

where $w_{T_{\rm react}}(r,\, t) = \sum_{\nu,\,\alpha} w^{\alpha}_{\nu_{\rm react}}(t)$ and T_T is the root mean square (rms) pulse length of the radiated field defined by

$$T_T = \sqrt{\mathcal{E}_T^{-1} \int_{-\infty}^{\infty} dt\, t^2\, P_{T_{\rm rad}}(t)}. \tag{21}$$

Without loss of generality it is assumed in this definition, that $P_{T_{\rm rad}}(t)$ is centered at $t = 0$, i.e., $\int_{-\infty}^{\infty} dt\, t\, P_{T_{\rm rad}}(t) = 0$.

A TD Q factor of the field with respect to the sphere a enclosing the antenna may now be defined as

$$Q_T(a) = 2\pi\, \frac{\mathcal{W}_T(a)}{\mathcal{E}_T}. \tag{22}$$

This general definition applies to *any* pulse shape with a finite energy. In particular, it reduces to the conventional definition for time-harmonic sources [4] given by $Q(a) = \omega\,(W_{\rm react}(a)/P_R)$, where $\omega = 2\pi/T$ is the radian frequency, P_R is the average radiative power, and $W_{\rm react}(a)$ is the average reactive energy stored in $r > a$. This monochromatic expression is obtained from (22) if $\mathcal{E}_T$ and $\mathcal{W}_T(a)$ are understood as the average values TP_R and $W_{\rm react}(a)$, respectively.

We seek now an expression for the *total* Q in terms of *modal* quantities. Such expression involves the *modal* Q (defined below) and the distribution of modal energies $\mathcal{E}^{\alpha}_{\nu}$ of (8) which depends on the specific realization. Such an expression explains how the total Q depends on the specific realization and can be used to compare different source realizations.

Following (22), the Q of a given mode $(\nu,\, \alpha)$ is defined as

$$Q^{\alpha}_{\nu}(a) = 2\pi\, \frac{\mathcal{W}^{\alpha}_{\nu}(a)}{\mathcal{E}^{\alpha}_{\nu}} \tag{23}$$

where $\mathcal{E}^{\alpha}_{\nu}$ are defined in (8), while the modal quantities $\mathcal{W}^{\alpha}_{\nu}(a)$ and T^{α}_{ν} are defined in analogy to the definitions in (20) and (21) above

$$\mathcal{W}^{\alpha}_{\nu}(a) = \frac{1}{T^{\alpha}_{\nu}} \int_a^{\infty} dr \int_{-\infty}^{\infty} dt\, w^{\alpha}_{\nu_{\rm react}}(r,\, t) \tag{24a}$$

$$T^{\alpha}_{\nu} = \sqrt{(\mathcal{E}^{\alpha}_{\nu})^{-1} \int_{-\infty}^{\infty} dt\, t^2 P^{\alpha}_{\nu_{\rm rad}}(t)}. \tag{24b}$$

Equation (23) may, therefore, be expressed as

$$Q^{\alpha}_{\nu}(a) = 2\pi\, \frac{\displaystyle\int_a^{\infty} dr \int_{-\infty}^{\infty} dt\, w^{\alpha}_{\nu_{\rm react}}(r,t)}{\displaystyle\left[\int_{-\infty}^{\infty} dt\, P^{\alpha}_{\nu_{\rm rad}}(r,\, t)\right]^{1/2} \left[\int_{-\infty}^{\infty} dt\, t^2 P^{\alpha}_{\nu_{\rm rad}}(t)\right]^{1/2}} \tag{25}$$

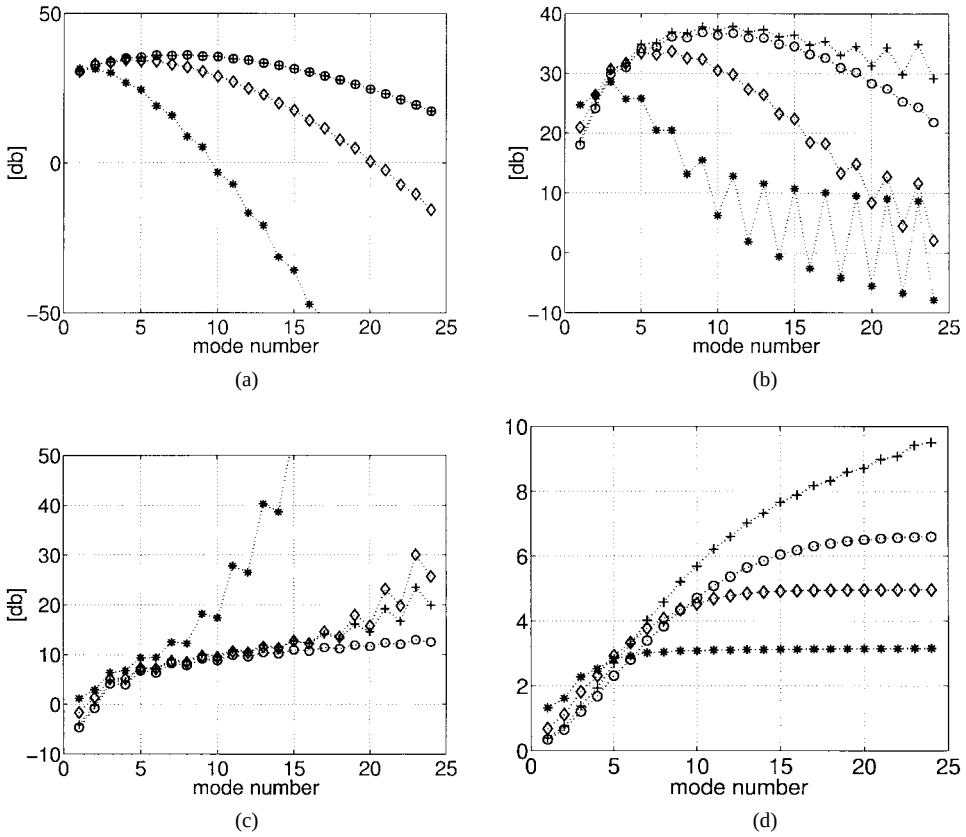

Fig. 3. Modal energies and Q for three disks with radii $a/cT = 3,\ 6$, and 9 (identified by $*$, $\Diamond$, and $\circ$, respectively). The $+$ signs describe the realization of the field due to the disk $a = 9cT$ by using a smaller source with $a = 8cT$. (a) The modal energies $\mathcal{E}_\nu$ calculated via (8). (b) The reactive modal energies $\mathcal{W}_\nu^\alpha$ calculated via (22). (c) The modal Q_ν^α calculated via (26). (d) The total Q_T calculated via.

where all terms have been previously expressed explicitly in terms of the multiple moments $M_\nu^\alpha(t)$.

Next, we note from the relations above that

$$\mathcal{E}_T = \sum_{\nu,\alpha} \mathcal{E}_\nu^\alpha, \quad T_T = \left[\sum_{\alpha,\nu} (\mathcal{E}_\nu^\alpha/\mathcal{E}_T) T_\nu^{\alpha 2}\right]^{1/2}$$
$$\mathcal{W}_T(a) = \sum_{\alpha,\nu} (T_\nu^\alpha/T_T)\mathcal{W}_\nu^\alpha(a), \quad \mathcal{W}_\nu^\alpha(a) = (2\pi)^{-1}\mathcal{E}_\nu^\alpha Q_\nu^\alpha(a). \tag{26}$$

Consequently, $Q_T(a)$ for the total field can be expressed in terms of the modal quantities

$$Q_T(a) = \frac{\sum_{\alpha,\nu} \mathcal{E}_\nu^\alpha T_\nu^\alpha Q_\nu^\alpha(a)}{\sqrt{\mathcal{E}_T \sum_{\nu,\alpha} \mathcal{E}_\nu^\alpha T_\nu^{\alpha 2}}}. \tag{27}$$

Equation (27) is the main result of this section and is the TD analog of (26) in [3].

B. Bounds on Source Realization

Equation (27) describes the total Q as a weighted sum of $\mathcal{E}_\nu^\alpha Q_\nu^\alpha(a)$, which from (26) are proportional to the modal reactive energies $\mathcal{W}_\nu^\alpha(a)$. Since $w_{\nu_{\text{react}}}^\alpha(r,t)$ is large for $r < ncT$ it follows from (24) that the series $Q_\nu^\alpha(a)$ diverges for $n > a/cT$ and, therefore, it should be compensated by an appropriate convergence of the modal radiative energies $\mathcal{E}_\nu^\alpha$ for $n > a/cT$. This later requirement restricts the directivity that can be achieved by physically realizable short-pulse sources.

Recalling (I.23), the TD radiation pattern $\mathbf{F}(t, \hat{\mathbf{r}})$ is uniquely realized by a series of multipoles $M_\nu^\alpha(t)$, identified by modal energies $\mathcal{E}_\nu^\alpha$. The series $\mathcal{E}_\nu^\alpha$ controls the directivity and is typically decaying for large n, say for $n > N$ where N is large for highly directive $\mathbf{F}$. Thus, it is required that the $Q_\nu^\alpha(a)$ will be bounded at least up to $n = N$ so that the series $\mathcal{E}_\nu^\alpha Q_\nu^\alpha(a)$ will be well behaved. This implies that a must be large so that $a > NcT$. Trying to synthesize the same radiation pattern with a smaller source, say $a_1 < a$, requires large modal reactive energies $\mathcal{W}_\nu^\alpha(a)$ for $a_1/cT < n < N$ leading to large $Q_T(a)$. This condition will be demonstrated in the example of Section V (see Fig. 3).

V. Example: Pulsed Radiation from a Circular Current Disk

The concept of the TD Q is demonstrate here for an example of a circular disk with radius a carrying a uniform distribution of pulsed current (see [1, fig. 2]). As in [1], we consider both "small" and "large" disks. The TD multipole moments have already been calculated in [1, sec. IV-A] where we also determined the number of the relevant terms as a function of the normalized disk size a/cT needed to calculate the field. Below, we shall explore the convergence of the modal series

for Q_T as well as the possible realization of the field due the "large" source by a smaller source.

Using the E- and H-modes multipole moments calculated in Section I-D. we calculate the radiative and reactive power flow (5), (6) and energy (14), (15), then the modal Q_ν^α (23), and, finally, the total Q_T (27), which represents the whole composition of modes.

Fig. 3 shows the energy constituents for three different disks with radii $a = 3cT$, $6cT$, and $9cT$ (indicated by $*$, $\Diamond$, and $\circ$, respectively). The subfigures depict, as a function of the mode index n: 1) the radiative energies of the modes $\mathcal{E}_\nu^\alpha$ of (8); 2) the modal reactive energies $\mathcal{W}_\nu^\alpha(a)$ of (26); 3) the modal $Q_\nu^\alpha = 2\pi\mathcal{W}_\nu^\alpha(a)/\mathcal{E}_\nu^\alpha Q_\nu^\alpha(a)/2\pi$ of (23); and 4) the total Q_T of (27) as a function of the number of modes used. Note from the modal energy distribution $\mathcal{E}_\nu^\alpha$ and from the results for the total quality factor Q_T that the relevant modes are those with $n \simeq 2a/cT$ (note also from (I.33) that the even and odd n correspond, in this special case, to E and H modes, respectively). Beyond this value, the modal energies are small and their contributions to the total Q are negligible.

Finally, we also explore in that figure the possible realization of the field corresponding to the $a = 9cT$ disk by using a smaller source bounded by $a = 8cT$ (the results are indicated by a $+$). The moments $M_\nu^\alpha(t)$ were taken to be those of the $a = 9cT$ case, leading to the same mode energies $\mathcal{E}_\nu^\alpha$ [compare the $*$ and the $+$ marks in subfigure (a)]. In subfigures 2)–4), however, one observes that the smaller source realization requires larger reactive energies $\mathcal{W}_\nu^\alpha(a)$ and modal $Q_\nu^\alpha(a)$ and, finally, to a slowly converging series for Q_T. The conclusion is that super resolution using short-pulse fields is not feasible since it involves large TD Q.

VI. Concluding Remarks

The near-field antenna characterization presented in this two-parts series has been derived entirely in the TD using the spherical transmission line representation. This representation applies for any spherically stratified medium and for any conical cross section, but it is used here explicitly for radiation in free-space where the mode functions are the scalar and vector spherical harmonics. The transmission line formulation decouples the transversal field structure (in θ, ϕ) from the radial propagation problem (in r, t) [see (I.6)], thus providing a systematic and physically transparent format to analyze the TD energy transmission mechanism in the radial direction.

The first part [1] dealt with the spherical field expansion. The radiated field outside the source domain is completely described by the TD multipole moment functions [see (I.17) or (I.19)], which are calculated directly from the TD current distribution via (I.22). Alternatively, the multipole moments can be determined by scanning the field on any sphere enclosing the source and in particular from the TD radiation pattern [see (I.23)]. Finally, using these relations we determined the convergence of the TD multipole expansion in both the near and far zones [1, sec. III-D]. In particular, it has been shown that the order of the relevant modes is $O(a/cT)$ where a is the source support and T is the excitation pulse length. Based on this observation it has been verified that the TD reactive fields practically vanish for $r > F = a^2/cT$ (F can be termed the TD Fresnel distance).

In this second part, we considered the energy content of the field. Using the spherical transmission line representation, the TD power-flow and the TD energy have been expressed in (2) and (10) as sums of modal quantities consisting of both radiative and reactive components [see (4) and (14)]. The radiative power is a positive pulse that propagates without distortion or decay, while the reactive power is a pulse with a zero mean [see (7)], strong in the near zone but vanishing in the far zone. At an early time, it is positive and builds up the local reactive energy, while at later time it is negative, representing energy discharge back to the source (see Section III-C).

Based on the reactive power flow and energy interpretation, we have introduced a TD Q factor (Section IV) to quantify the radiation efficiency of the pulsed antenna. It is defined in (22) as the ratio between the time-averaged reactive energy surrounding the antenna and the total radiation energy. Next, in (27) we derived and expressed the (total) antenna Q as a weighted sum of modal quantities: the modal Q's and the modal energies $\mathcal{E}_\nu^\alpha$. Since $Q_\nu^\alpha(a)$ diverge for $n > a/cT$, convergence of (27) requires a stronger convergence of $\mathcal{E}_\nu^\alpha$. This weak excitation of the higher order modes sets a limit on the TD radiation pattern and directivity that can be achieved by physically realizable short-pulse antennas.

Finally, the TD concepts discussed above were demonstrated for a circular disk carrying a pulsed current distribution (Section V). This configuration has been analyzed first in [1], where the emphasis was the calculation of the TD multipole functions and the field. To check the calculations we have compared the radiation pattern calculated via the multipole expansion with a closed-form expression obtained independently via the TD plane wave spectrum and the slant stack transform integral (I.34), and obtained a full agreement. The numerical results of [1] have been utilized in this second part to explore the TD reactive energy around the antenna and to calculate the TD Q. Specifically, it has been shown that Q, as well as the number of the relevant modes needed to model the TD field, is governed by the ratio a/cT. Trying to synthesize the TD radiation pattern of a large antenna with a smaller one results in rapidly diverging Q and a nonrealizable source distribution. Thus, trying to achieve super resolution using short-pulse antennas is probably not feasible.

Appendix
Proof of (7)

The proof of (7) in (18) has been based on the energy conservation relation. Here we shall verify this property by analyzing the expression for $P_{\nu_{\text{react}}}^\alpha(r, t)$. Using (I.22) for the multipole moments from in (5) and (6) and inserting the result into (8), we obtain

$$\mathcal{E}_\nu^\alpha = \eta^{\pm 1}(-1)^{N^\alpha} \sum_{p=0}^{2n+1} \left(\frac{c}{r}\right)^p A_p \partial_\xi^{2N^\alpha - p} \mathcal{R}_{m_\nu^\alpha}(\xi)|_{\xi=0} \quad \text{(28a)}$$

$$\text{with} \qquad A_p = \sum_{q=q_{\min}}^{q_{\max}} (-1)^q a_{n,\,p-q} b_{n,\,q} \quad \text{(28b)}$$

where $q_{\min,\max}$ as defined in (6). In (8) $\mathcal{R}_{m_\nu^\alpha}(\xi) = \int dt\, m_\nu^\alpha(t) m_\nu^\alpha(t-\xi)$ is the autocorrelation of $m_\nu^\alpha(t)$.

The $p = 0$ term in (28a) has the form $\eta^{\pm 1}(-1)^{N^\alpha}\, \partial_\xi^{2N^\alpha} \mathcal{R}_{m_\nu^\alpha}(\xi)|_{\xi=0}$ and is readily recognized as $\int_{-\infty}^{\infty} dt\, P_{\nu_{\rm rad}}^\alpha(r,t)$ of (8). The remaining series, the contribution of the reactive power, vanishes term by term. For p even, the coefficients A_p vanish since from (I.14) and (I.16) the terms in the q summation for A_p in (28b) cancel each other. For p odd $\partial_\xi^{2N^\alpha - p} \mathcal{R}_{m_\nu^\alpha}(\xi)|_{\xi=0} = 0$ since $\mathcal{R}_{m_\nu^\alpha}(\xi)$ is an even function. This proves (7).

REFERENCES

[1] A. Shlivinski and E. Heyman, "Time domain near field analysis of short pulse antennas—Part I: Spherical wave (multipole) expansion," *IEEE Trans. Antennas Propagat.*, this issue, pp. 271–279.

[2] R. F. Harrington, "On the gain and bandwidth of directional antennas," *IRE Trans. Antennas Propagat.*, vol. AP-6, pp. 219–225, July 1958.

[3] ———, "Effect of antenna size on gain, bandwidth and efficiency," *J. Res. Nat. Bureau Standards*, vol. 64D, pp. 1–12, 1960.

[4] R. E. Collin and S. Rothschild, "Evaluation of antenna Q," *IRE Trans. Antennas Propagat.*, vol. AP-12, pp. 23–27, Jan. 1964.

[5] R. L. Fante, "Quality factor of general ideal antennas," *IEEE Trans. Antennas Propagat.*, vol. AP-17, pp. 151–155, 1969.

[6] J. E. Hansen, *Spherical Near-Field Antenna Measurements.* London, U.K.: Peter Peregrinus, 1988.

Amir Shlivinski, for a photograph and biography, see this issue, p. 279.

E. Heyman, for a biography, see p. 528 of the May 1995 issue of this TRANSACTIONS.